

Transport properties of $\text{La}_{1.85-x}\text{Sr}_{0.15+x}\text{Cu}_{1-x}\text{M}_x\text{O}_y$ ($M = \text{Co}, \text{Ga}$)

Xu Gaojie

Structure Research Laboratory University of Science and Technology of China, Hefei, Anhui 230026, People's Republic of China
and Department of Chemistry, University of Science and Technology of China, Hefei, Anhui 230026, People's Republic of China

Mao Zhiqiang, Jin Hao, Yan Hongjie, Wang Bin, and Liu Dengpan

Structure Research Laboratory, University of Science and Technology of China, Hefei, Anhui 230026, People's Republic of China

Zhang Yuheng

Structure Research Laboratory, University of Science and Technology of China, Hefei, Anhui 230026, People's Republic of China
and Chinese Center of Advanced Science and Technology (World Laboratory), P.O. Box 8730, Beijing, People's Republic of China

(Received 4 August 1998; revised manuscript received 19 October 1998)

The transport properties of double doped samples $\text{La}_{1.85-x}\text{Sr}_{0.15+x}\text{Cu}_{1-x}\text{Co}_x\text{O}_y$ ($0 \leq x \leq 1.0$) are investigated by means of resistivity and thermoelectric power (TEP). It is found that with Co doping, the lattice parameter a increases first and then decreases as $x \geq 0.6$, where the resistivity and thermoelectric power exhibit a corresponding anomaly. Analyzing the discrepancy of the thermal activation energy derived from the resistivity and TEP, we find that the transport mechanism can be understood in terms of the polaron model. The corresponding Ga doped system is also analyzed as a comparison. Another interesting phenomenon is the different change of the broad peaks in S - T curves between Co and Ga doped systems, which is discussed according to the change of spin correlation. [S0163-1829(99)02717-4]

INTRODUCTION

It is known that one characteristic of the copper-oxide superconductors is the close relation between the spin correlation and superconductivity. Recently there has been renewed interest in the normal state (NS) properties since many researchers believed that the study of NS transport properties could provide important clues to the basic mechanism responsible for superconductivity. Elemental doping is a very effective means in probing the local electronic and magnetic properties as well as studying the relation between spin correlation and transport properties. A more ideal system for studying the effect of chemical substitution on NS properties is the La214 system, which possesses a single CuO_2 plane and one Cu site. Studying this system avoids any contribution to NS transport properties from the charge reservoir in the nonsuperconductive intergrowth layers. There have been many reports on the magnetism, transport properties, and superconductivity of $\text{La}_{2-x}\text{Sr}_x\text{CuO}_{4+\delta}$ superconductors doped with $3d$ and sp metals (Fe, Mn, Co, Ni, Zn, Ga, Al, etc.).¹⁻⁶ Xiao *et al.*² investigated the effective moment of different cations doped in the La214 system and proposed a magnetic pair-breaking effect for the suppression of T_c . Ishikawa *et al.*⁷ analyzed the change of spin correlation energy with elemental doping and pointed out that the Co doping increases the spin correlation energy, while Ga and Zn doping decreases the energy. The Ni doping has the least impact on the spin correlation. Therefore, an investigation of the transport properties of systems doped with Co, Ga, and Ni would be helpful to reveal the relation between spin correlation and transport properties. We have systematically investigated the transport properties of $\text{La}_{1.85}\text{Sr}_{0.15}\text{Cu}_{1-x}\text{Ni}_x\text{O}_{4+\delta}$ ($0 \leq x \leq 1.0$) and found evidence for polaronic transport in this solid solution series.⁸ The size

of polaron decreases rapidly as $x(\text{Ni}) > 0.3$ and the contribution of polarons to transport also becomes dominant as $x > 0.3$.

In order to widely compare the transport properties between different systems doped with $3d$ elements, recently we prepared double-doped samples $\text{La}_{1.85-x}\text{Sr}_{0.15+x}\text{Cu}_{1-x}\text{Co}_x\text{O}_y$ ($0 \leq x \leq 1$) and $\text{La}_{1.85-x}\text{Sr}_{0.15+x}\text{Cu}_{1-x}\text{Ga}_x\text{O}_y$ ($0 \leq x \leq 0.4$). The decrease of carrier concentration induced by Co or Ga doping is compensated nearly by more Sr doping in the two systems. So the change of transport properties should be dominated mainly by the varying characteristic of spin correlation. In this paper we present the transport properties of the two systems and compare them with other systems, and then discuss their discrepancy in terms of spin correlation and the polaron model.

EXPERIMENT

Samples of $\text{La}_{1.85-x}\text{Sr}_{0.15+x}\text{Cu}_{1-x}\text{Co}_x\text{O}_y$ ($0 \leq x \leq 1.0$) and $\text{La}_{1.85-x}\text{Sr}_{0.15+x}\text{Cu}_{1-x}\text{Ga}_x\text{O}_y$ ($0 \leq x \leq 0.4$) systems were prepared by means of a conventional solid state reaction method using high-purity powders of La_2O_3 , CuO , Co_2O_3 , Ga_2O_3 , and SrCO_3 . Since La_2O_3 is strongly hygroscopic, it was dried at 850°C in a furnace for 5 h before weighing. Initially the appropriate mixture of these powders was well ground and preheated in air at 1070 – 1300°C for 40 h with an intermediate grinding. Then the mixture was reground and pressed into disk-shaped pellets. The pellets were sintered in air at 1080 – 1320°C for one day. In order to ensure that the samples were homogeneous, the pellets were pulverized and repressed into pellets, sintered at 1080 – 1320°C for another day, and finally cooled down to 800°C in the furnace and kept at the temperature in air for 40 h.

X-ray diffraction (XRD) analysis was carried out by a

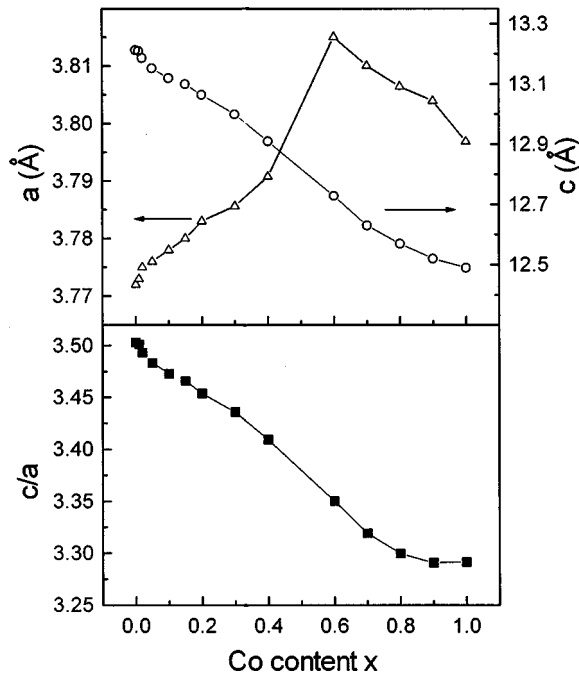


FIG. 1. Lattice parameters a and c and the ratio of c/a as a function of Co content in $\text{La}_{1.85-x}\text{Sr}_{0.15+x}\text{Cu}_{1-x}\text{Co}_x\text{O}_y$ system.

Rigaku-D/max- γA diffractometer using high-intensity $\text{Cu-K}\alpha$ radiation to screen for the presence of impurity phase and the changes in structure. The lattice parameters were determined from the d values of XRD peaks by a standard least-squares refinement method. The oxygen content of the Co doped samples was determined by iodometric titration with an error of 0.02. Resistivity as a function of temperature for all the prepared samples was measured using a standard four-probe method in a closed-cycle helium cryostat. The thermoelectric power $S(T)$ was measured by a differential method. The temperature at two ends of the measured sample was controlled automatically within a precision of 0.01 K, and the temperature gradient between both ends of the sample was 2 K. The emf of the sample was indicated by a Keithley 182 Nanovoltmeter with an error of the thermoelectric power (TEP) measurement of smaller than $0.1 \mu\text{V/K}$.

RESULTS

XRD analysis shows the formation of single-phase products with a tetragonal K_2NiF_4 structure for all the prepared samples. The result of oxygen content measurement of samples $\text{La}_{1.85-x}\text{Sr}_{0.15+x}\text{Cu}_{1-x}\text{Co}_x\text{O}_y$ shows that for the samples with $x=0, 0.1, 0.2, 0.4, 0.6, 0.8$, and 1.0 , the y is 4.00, 4.00, 4.00, 4.00, 3.99, 3.99, and 3.98, respectively, which implies that the simultaneous Sr doping nearly compensates the change of carrier concentration induced by Co (or Ga) doping.

The lattice parameters a and c and the ratio of c/a for all Co-doped samples as a function of Co content x are shown in Fig. 1. An anomalous change of lattice parameters can be clearly observed, i.e., with increasing Co content the parameters a increases first, and then decreases as $x \geq 0.6$, while the parameter c decreases monotonously with increasing x . The

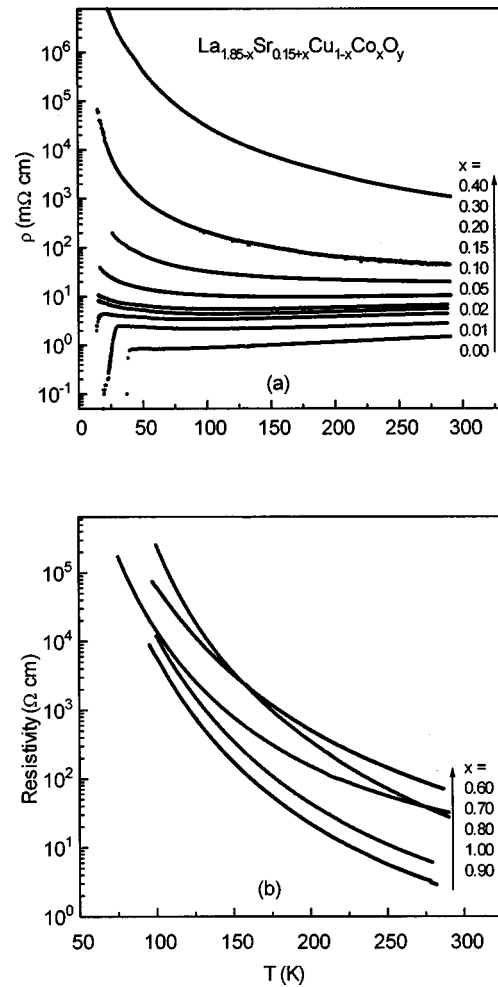


FIG. 2. Temperature dependence of resistivity for samples $\text{La}_{1.85-x}\text{Sr}_{0.15+x}\text{Cu}_{1-x}\text{Co}_x\text{O}_y$.

c/a value is nearly unchanged for $x \geq 0.9$.

Figures 2(a) and 2(b) show the temperature dependence of resistivity for the $\text{La}_{1.85-x}\text{Sr}_{0.15+x}\text{Cu}_{1-x}\text{Co}_x\text{O}_y$ solid solution series. With increasing Co content, the T_c decreases rapidly and the superconductivity disappears for the samples with $x > 0.02$, which is consistent with a previous report.² From Fig. 2, one can also see that the samples with $x \leq 0.15$ exhibit metal-like behavior at high temperatures, while the samples with $x \geq 0.2$ show semiconductinglike behavior over all the measured temperature region. Figure 4 shows the room-temperature resistivity (290 K) as a function of Co content. It shows that the resistivity value [$\rho(290)$] increases rapidly with Co content for $x \leq 0.6$ and then decreases for $x > 0.6$. A maximum for $\rho(290)$ is reached at $x = 0.6$.

Figures 3(a), 3(b), and 3(c) show the variation of S with T for $\text{La}_{1.85-x}\text{Sr}_{0.15+x}\text{Cu}_{1-x}\text{Co}_x\text{O}_y$ samples. For the Co-free sample $\text{La}_{1.85}\text{Sr}_{0.15}\text{CuO}_y$, both the value and temperature dependence of the TEP is analogous to the result reported previously.⁹ For the samples with $x \leq 0.15$, two obvious changes in the TEP can be observed in Fig. 3(a). One is that the TEP value decreases gradually with the increase of Co content, and the other is that the temperature (T_m) corresponding to the broad maximum (peak) in S - T curve increases. For the samples with $0.2 \leq x \leq 0.6$, the room temperature TEP value increases rapidly with the further

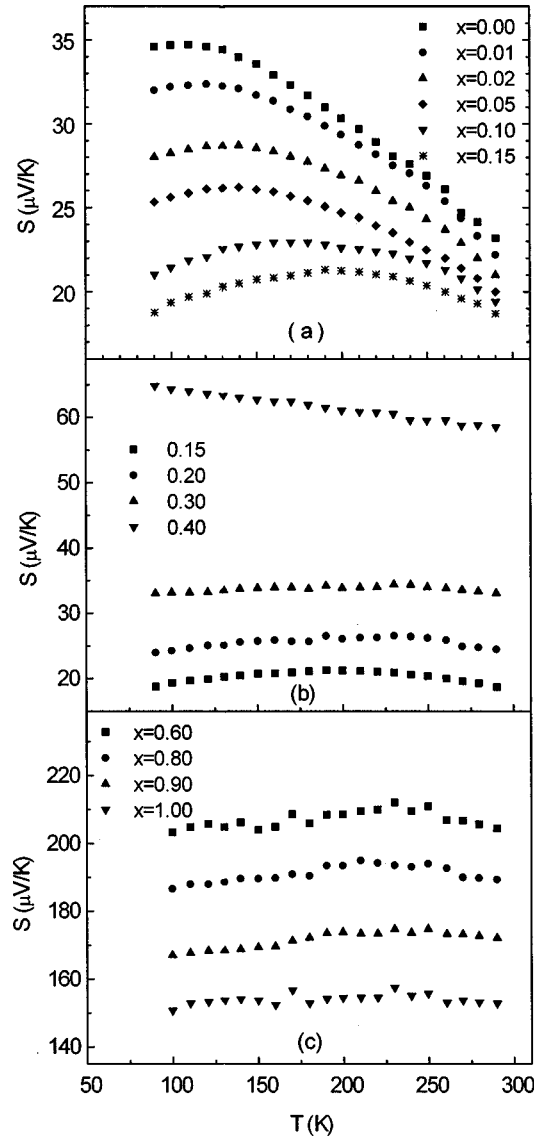


FIG. 3. (a)–(c) Temperature dependence of TEP for samples $\text{La}_{1.85-x}\text{Sr}_{0.15+x}\text{Cu}_{1-x}\text{Co}_x\text{O}_y$. (a) $0 \leq x \leq 0.15$, (b) $0.15 \leq x \leq 0.4$, (c) $0.6 \leq x \leq 1.0$.

increase of Co content and the $S(T)$ shows a very weak temperature dependence. As $x > 0.6$ the TEP decreases gradually with x . Figure 4 shows the room temperature TEP, $S(290)$, as a function of Co content. A maximum of $S(290)$ at $x = 0.6$ is also seen clearly.

To contrast the transport properties of the Co-doped system with the Ni series, we examined the possibility of polaron transport for the Co series from the thermal activation energy derived from resistivity and TEP. One knows that for a thermal activated conduction process, the resistivity and TEP would show the following temperature dependence, respectively:

$$\rho(T) = \rho_0 \exp(\varepsilon_a/kT), \quad (1)$$

$$S(T) = \pm (k/e)(\varepsilon_a/kT + A), \quad (2)$$

where the + and – sign holds for hole-type and electron-type conduction and the constant A is determined by the energy dependence of scattering time. In terms of Eqs. (1)

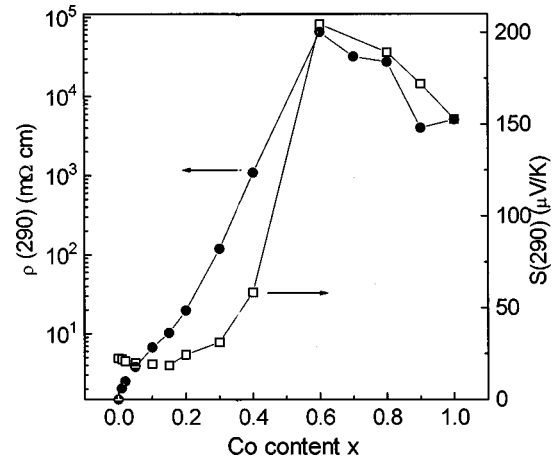


FIG. 4. Room-temperature resistivity $[\rho(290)]$ and TEP $[S(290)]$ as a function of Co content x for the $\text{La}_{1.85-x}\text{Sr}_{0.15+x}\text{Cu}_{1-x}\text{Co}_x\text{O}_y$ system.

and (2), we plotted $\ln(\rho)$ and S as a function of $1/T$ for $\text{La}_{1.85-x}\text{Sr}_{0.15+x}\text{Cu}_{1-x}\text{Co}_x\text{O}_y$ in Figs. 5(a) and 5(b). The activation energy ε_a derived from the slope of straight lines at high temperature is summarized in Fig. 6. Here, we use ε_a^p

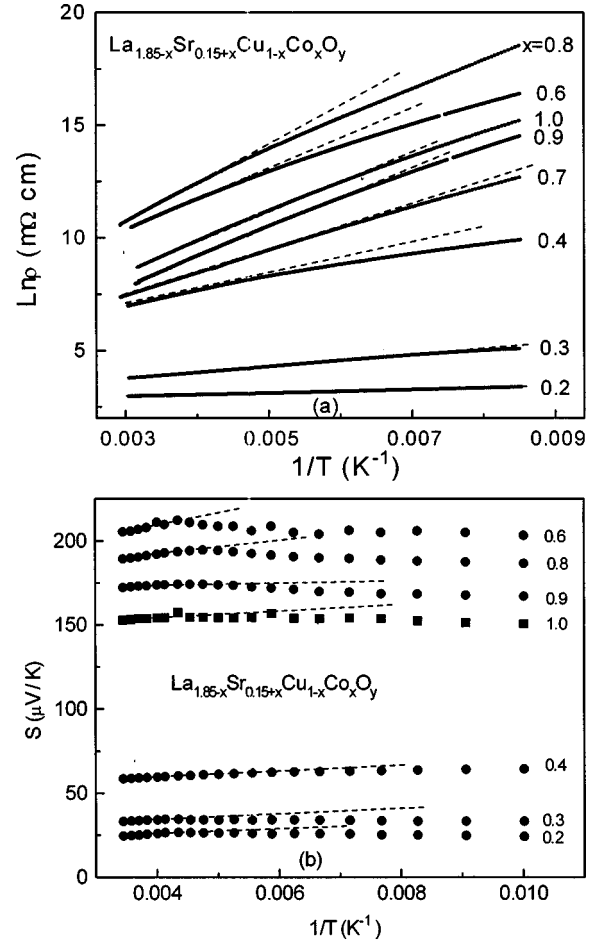


FIG. 5. (a) Resistivity in logarithmic scale vs $1/T$ for samples $\text{La}_{1.85-x}\text{Sr}_{0.15+x}\text{Cu}_{1-x}\text{Co}_x\text{O}_y$ ($x \geq 0.2$). (b) TEP vs $1/T$ for samples $\text{La}_{1.85-x}\text{Sr}_{0.15+x}\text{Cu}_{1-x}\text{Co}_x\text{O}_y$ ($x \geq 0.2$). The straight dashed lines in the figures are the linear fit at the high temperatures and give the thermal activation energy ε_a^p and ε_a^S in Fig. 6.

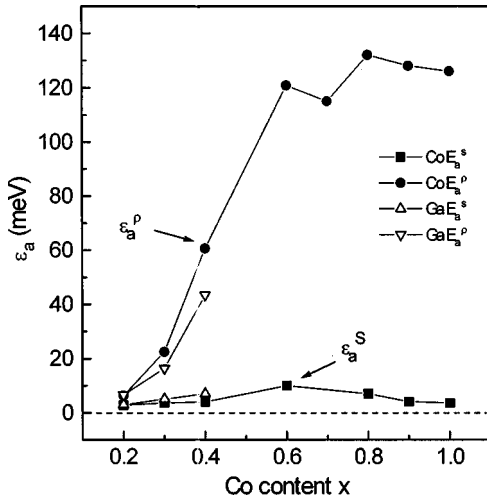


FIG. 6. Thermal activation energy (ϵ_a^p and ϵ_a^S) derived from the resistivity and TEP vs the Co or Ga concentration x for samples $\text{La}_{1.85-x}\text{Sr}_{0.15+x}\text{Cu}_{1-x}\text{M}_x\text{O}_y$ ($M = \text{Co}, \text{Ga}$).

and ϵ_a^S to denote the activation energy derived from resistivity and TEP, respectively. As seen in Fig. 6, the ϵ_a^p increases rapidly with Co content for $x < 0.6$ and slowly as $x > 0.6$. While ϵ_a^S accrues slowly first with x for $x \leq 0.6$ and then decreases slowly with further increasing x . Here the noteworthy point is that for the $x = 0.2$ sample, ϵ_a^p is nearly the same as ϵ_a^S , while ϵ_a^p is systematically larger than ϵ_a^S for the samples with $x > 0.2$. The difference between ϵ_a^p and ϵ_a^S , $\epsilon_a^p - \epsilon_a^S$, enhances progressively with increasing Co content, and reaches a maximum, 124.7 meV, at $x = 0.8$. Further increase of Co content for $x > 0.8$ does not give rise to more increase in $\epsilon_a^p - \epsilon_a^S$.

In order to compare the change of TEP between magnetic and nonmagnetic ions doping, Figs. 7(a) and 7(b) give the temperature-dependent TEP for $\text{La}_{1.85-x}\text{Sr}_{0.15+x}\text{Cu}_{1-x}\text{Ga}_x\text{O}_y$ ($0 \leq x \leq 0.4$) samples. The room-temperature TEP $S(290)$ decreases gradually with increasing x for the samples with $x \leq 0.15$ and then increases for $x \geq 0.2$, which is similar to that of the Co-doped samples. For the broad peak in the S - T curve, however, an obvious difference between Co and Ga doped systems can be observed, i.e., the T_m for the Ga doped system remains unchanged, which is similar to that of the Zn doped La214 system.¹⁰ The corresponding activation energy derived from the resistivity and the TEP of Ga doped system is also shown in Fig. 6. Obviously the value of $\epsilon_a^p - \epsilon_a^S$ for Ga doped samples is smaller than that of Co doped samples.

DISCUSSION

The above analysis of the activation energy (see Fig. 6) shows that a great difference between ϵ_a^S and ϵ_a^p exists in the Co-doped series. This discrepancy can be understood in terms of the small polaron model. In this model, the small polarons are the self-localized states which are induced by the magnetic coupling between magnetic ions and hole spins.¹¹⁻¹³ From the small polaron model, it can be deduced that the polaron formation energy ϵ_p is twice as much as the difference between ϵ_a^S and ϵ_a^p , i.e., $\epsilon_p = 2(\epsilon_a^p - \epsilon_a^S)$. From Fig. 6 one can see that with the increase of Co content the

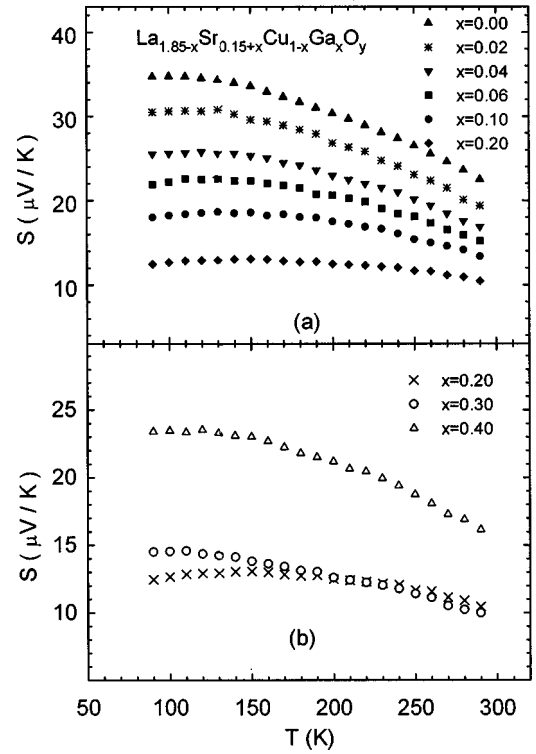


FIG. 7. The TEP as a function of temperature for the samples $\text{La}_{1.85-x}\text{Sr}_{0.15+x}\text{Cu}_{1-x}\text{Ga}_x\text{O}_y$ ($0 \leq x \leq 0.4$).

formation energy (ϵ_p) of polarons increases rapidly as $x < 0.6$ and the ϵ_p reaches 221 meV for the $x = 0.6$ sample. This value is close to the ϵ_p value 240 meV determined by optical conducting measurements for $\text{La}_{1.85}\text{Sr}_{0.15}\text{NiO}_{4+\delta}$,¹² and 204 and 220 meV, observed in $\text{La}_{2/3}\text{Ca}_{1/3}\text{MnO}_3$ (Ref. 14) and $\text{La}_{1.85}\text{Sr}_{0.15}\text{Cu}_{1-x}\text{Ni}_x\text{O}_4$ (Ref. 8), respectively. This suggests that the charge carriers in the samples with $x \geq 0.6$ substantially have the characteristic of small polarons. However, this value is much larger than the 60 meV detected by an optical conductivity measurement in $\text{La}_{1.85}\text{Sr}_{0.15}\text{CuO}_{4+\delta}$ and smaller than the 350 meV obtained in the Sr doped LaCoO_3 (ABO₃ type) system.¹⁵ This kind of difference originates from the different polaron characteristics. For example, in $\text{La}_{1.85}\text{Sr}_{0.15}\text{CuO}_{4+\delta}$ the ϵ_p is 60 meV, which is only a quarter of the ϵ_p in $\text{La}_{1.85}\text{Sr}_{0.15}\text{NiO}_4$; however, the polaron size of the former is almost 10 times as much as the latter. The study of $\text{La}_{1.85}\text{Sr}_{0.15}\text{CuO}_{4+\delta}$ and $\text{La}_{1.85}\text{Sr}_{0.15}\text{Cu}_{1-x}\text{Ni}_x\text{O}_4$ systems suggested that the formation energy of polarons is closely related to the size of polaron. The polaron generally tends to expand with the reduction of formation energy. Therefore for the samples $\text{La}_{1.85-x}\text{Sr}_{0.15+x}\text{Cu}_{1-x}\text{Co}_x\text{O}_y$ with lower doping level, the formation energy of polarons is small and the size of polarons is large. More Co doping ($x > 0.4$) leads to a contraction in polaron size. Obviously the Co doping favors the formation and stabilization of small polarons.

For the Ga doped system, a difference between ϵ_a^p and ϵ_a^S also exists, which may be that Ga doping favors the localization of the charge carrier. The coupling between Cu^{2+} and localized hole spins exhibits polaronic characteristic. Since Ga^{3+} is not a magnetic ion, it cannot couple with hole spins, which may be the origin of the different $\epsilon_a^p - \epsilon_a^S$ between Co and Ga doped samples. Unfortunately, we cannot obtain Ga

doped samples with $x > 0.45$, so any further comparison is hampered.

The analysis of lattice parameters indicates that Co doping induces parameter a to increase first and then decrease as $x > 0.6$, which is different from the Ni doped La214 system. The anomalous changes in the room-temperature resistivity and TEP (as shown in Fig. 4) may originate from the change of structure.

Another phenomenon that should be noted is that the TEP for Co and Ga doped samples with low doping level shows a different change, i.e., Co doping leads to the broad peak in the S - T curve shifting up to high temperature, while Ga doping does not change T_m . The origin and change of the temperature-dependent broad peaks in TEP curves for high- T_c superconductors have attracted wide attention. Many models were proposed to account for the origin.^{16–19} Up to now, however, no consensus was achieved. Previous experimental results showed that the shift of the peaks is accompanied by the change of carrier concentration. For examples, in the systems of $\text{La}_{2-x}\text{Sr}_x\text{CuO}_y$,²⁰ $\text{Bi}_2\text{Sr}_{2-2y}\text{La}_{2y}\text{CuO}_{6+x}$, $\text{Nd}_{1+z}\text{Ba}_{2-y}\text{Cu}_3\text{O}_{6+x}$,²¹ and $(\text{Yb}, \text{Ca})(\text{BaSr})_2\text{Cu}_3\text{O}_z$ ($6.1 \leq z \leq 6.78$),²² the humps all shift to high temperature with decreasing carrier concentration. It appears to mean that the variation of the humps is related to carrier concentration. However, this is obviously not the case for the Co doped system, see Fig. 3(a). It is known that Co possesses a unfilled $3d$ electrons. These electrons can form strong hybridization with charge carriers in CuO_2 planes and strengthen the spin correlation of the conducting planes, while Ga (or Zn) has

full $3d$ electrons and can only form weak d - p hybridization with oxygen. Ga doping mainly introduces spin vacancy and weakens the spin correlation. In fact, previously experimental results had demonstrated that Co doping increases spin correlation energy, while both Ga and Zn doping decrease this energy.⁷ In addition, the decrease of carrier concentration would enhance spin correlation. Therefore, based on all the experimental results mentioned above it is suggested that the changes of hybridization state and spin correlation for Co and Ga doped systems are the main reason for the shift of broad peak in the TEP for $x \leq 0.15$.

In summary, the structure and transport properties of $\text{La}_{1.85-x}\text{Sr}_{0.15+x}\text{Cu}_{1-x}\text{Co}_x\text{O}_y$ ($0 \leq x \leq 1$) were investigated. It is found that Co doping leads to an anomalous change in the crystal structure at $x = 0.6$, which induces corresponding changes in the transport properties. Based on the difference of ε_a^p and ε_a^s , we analyze the possibility of polaronic conduction and suggest that Co doping favors the stabilization of small polarons. The different changes of the broad peak in S - T curves for Co and Ga doped samples were observed, which may result from the different spin correlation.

ACKNOWLEDGMENTS

This work was supported by the National Center for Research and Development on Superconductivity, the National Natural Science Foundation of China, Grant No. 59625205, and the China Postdoctoral Science Foundation.

- ¹Marta Z. Cieplak, S. Guha, H. Kojima, P. Lindenfeld, Gang Xiao, J. Q. Xiao, and C. L. Chien, Phys. Rev. B **46**, 5536 (1992).
- ²Gang Xiao, Marta Z. Cieplak, J. Q. Xiao, and C. L. Chien, Phys. Rev. B **42**, 8752 (1990).
- ³Marta Z. Cieplak, A. Sienkiewicz, F. Mila, S. Guha, Gang Xiao, J. Q. Xiao, and C. L. Chien, Phys. Rev. B **48**, 4019 (1993).
- ⁴B. I. Kochelaev, L. Kan, B. Elschner, and S. Elschner, Phys. Rev. B **49**, 13 106 (1994).
- ⁵H. Harashina, T. Nishikawa, T. Kiyokura, S. Shamoto, M. Sato, and K. Kakurai, Physica C **212**, 142 (1993).
- ⁶J. Takeda, T. Nishikawa, and M. Sato, Physica C **231**, 293 (1994).
- ⁷N. Ishikawa, N. Kuroda, H. Ikeda, and Yoshizaki, Physica C **203**, 284 (1992).
- ⁸Mao Zhiqiang, Xu Gaojie, Wang Bin, Yan Hongjie, Qiu Xueyin, and Zhang Yuheng, Phys. Rev. B **58**, 15116 (1998).
- ⁹J.-S. Zhou and J. B. Goodenough, Phys. Rev. B **51**, 3104 (1995).
- ¹⁰J. L. Tallon, J. R. Cooper, P. S. I. P. N. De Silva, G. V. M. Williams, and J. W. Loram, Phys. Rev. Lett. **77**, 1191 (1996).
- ¹¹V. I. Anisimov, M. A. Korotin, J. Zaanen, and O. K. Andersen, Phys. Rev. Lett. **68**, 345 (1992).
- ¹²X.-X. Bi and P. C. Eklund, Phys. Rev. Lett. **70**, 2625 (1993).
- ¹³S.-W. Cheong, H. Y. Hwang, C. H. Chen, B. Batlogg, L. W. Rupp, Jr., and S. A. Carter, Phys. Rev. B **49**, 7088 (1994).
- ¹⁴M. Jaime, M. B. Salamon, M. Rubinstein, R. E. Treece, J. S. Horwitz, and D. B. Chrisey, Phys. Rev. B **54**, 11 914 (1996).
- ¹⁵R. Muhlstroh and H. G. Reik, Phys. Rev. **162**, 703 (1967).
- ¹⁶A. J. Millis, H. Monien, and D. Pines, Phys. Rev. B **42**, 167 (1990).
- ¹⁷X. Schrieffer, X. G. Wen, and S. C. Zhang, Phys. Rev. Lett. **60**, 944 (1988); Phys. Rev. B **39**, 11 663 (1989).
- ¹⁸N. Nagaosa and P. A. Lee, Phys. Rev. Lett. **64**, 2450 (1990).
- ¹⁹P. W. Anderson, Science **215**, 1196 (1987).
- ²⁰J. Takeda, T. Nishikawa, and M. Sato, Physica C **231**, 293 (1994).
- ²¹F. Devaux, A. Manthiram, and J. B. Goodenough, Phys. Rev. B **41**, 8723 (1990).
- ²²Kiyotaka Matsuura, Takahiro Wada, Yuji Yaegashi, S. Tajima, and H. Yamauchi, Phys. Rev. B **46**, 11 923 (1992).